

Supporting information

Near Infra-Red Luminescent Osmium Labelled Gold Nanoparticles for Cellular Imaging and Singlet Oxygen Generation

Luke S. Watson,^a Joseph Hughes,^a Salma T. Rafik,^{b, c} Asier R. Muguruza,^a Patricia M. Girio,^{a, e} Sarah O. Akponasa,^{a, d} Garret Rochford,^d Alexander J. MacRobert,^b Nikolas J. Hodges,^d Elnaz Yaghini^b and Zoe Pikramenou^a

^a School of Chemistry, ^e Doctoral Training Centre in Physical Sciences for Health, University of Birmingham, Edgbaston, B15 2TT, United Kingdom.

^b Dept. of Surgical Biotechnology, Faculty of Medical Sciences, University College London, London, United Kingdom.

^c Department of Clinical Pharmacology, Faculty of Medicine, Alexandria University, Alexandria 21516, Egypt.

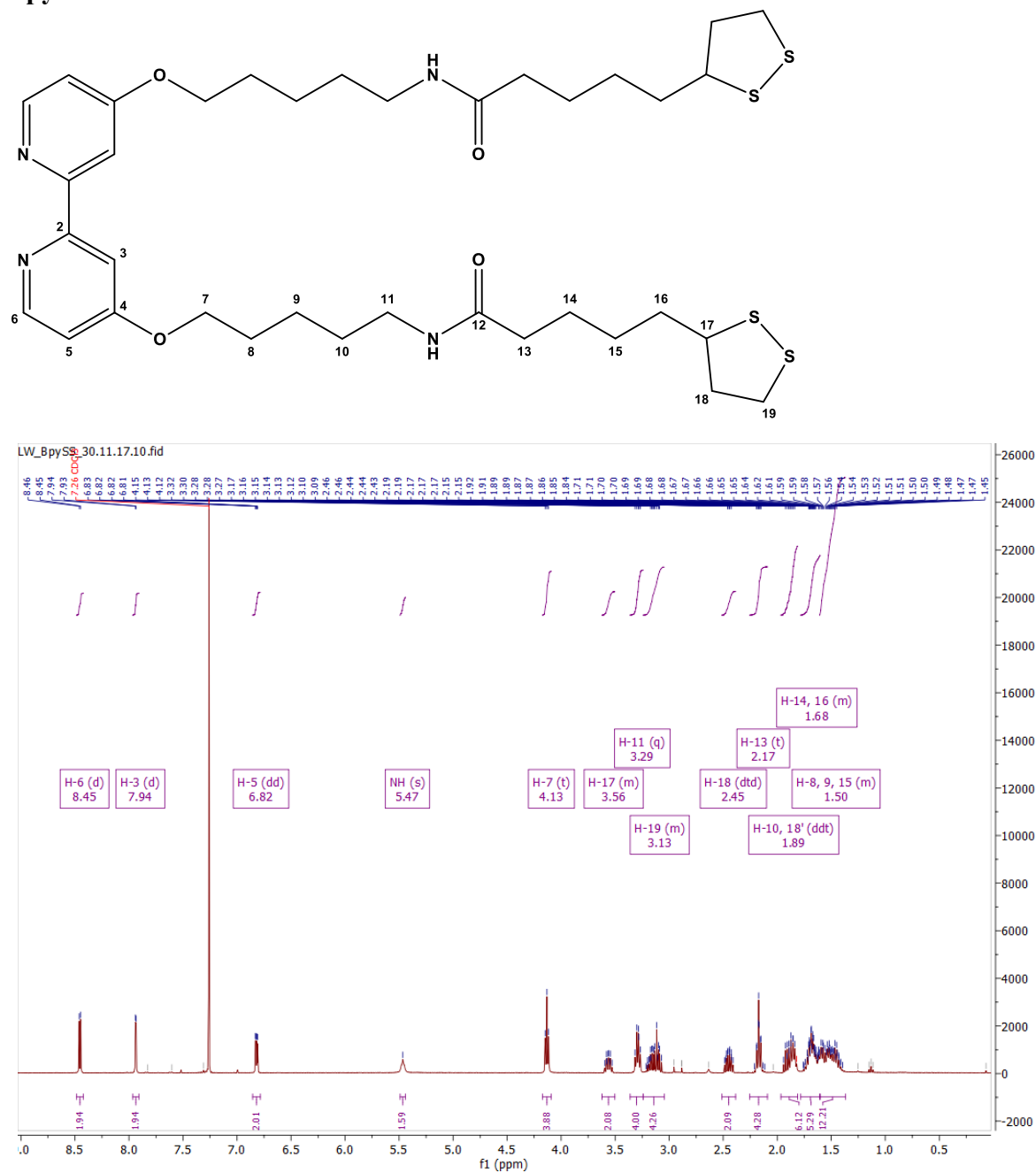
^d School of Biosciences, University of Birmingham, Edgbaston, B15 2TT, United Kingdom.

*Corresponding author: z.pikramenou@bham.ac.uk

This file includes:

| | Page number |
|--|-------------|
| Table of Contents | |
| BpySS Characterisation | S 2 |
| Os(phen) ₂ Cl ₂ Characterisation | S 4 |
| OsPhenSS Characterisation | S 5 |
| Photophysical Characterisation of OsPhenSS in presence of fluorosurfactant | S10 |
| Data summary of gold nanoparticles' characterisation data | S11 |
| Photophysical characterisation of OsPhenSS gold nanoparticles | S13 |
| Cell viability assays of OsPhenSS gold nanoparticles in live A549 cells | S13 |
| Additional confocal images of z-stacks of OsPhenSS•AuNP25 | S15 |
| Calculation of number (<i>N</i>) of gold atoms per nanoparticle | S17 |

BpySS Characterisation

Figure S1. ^1H NMR spectrum of BpySS in CDCl_3 .

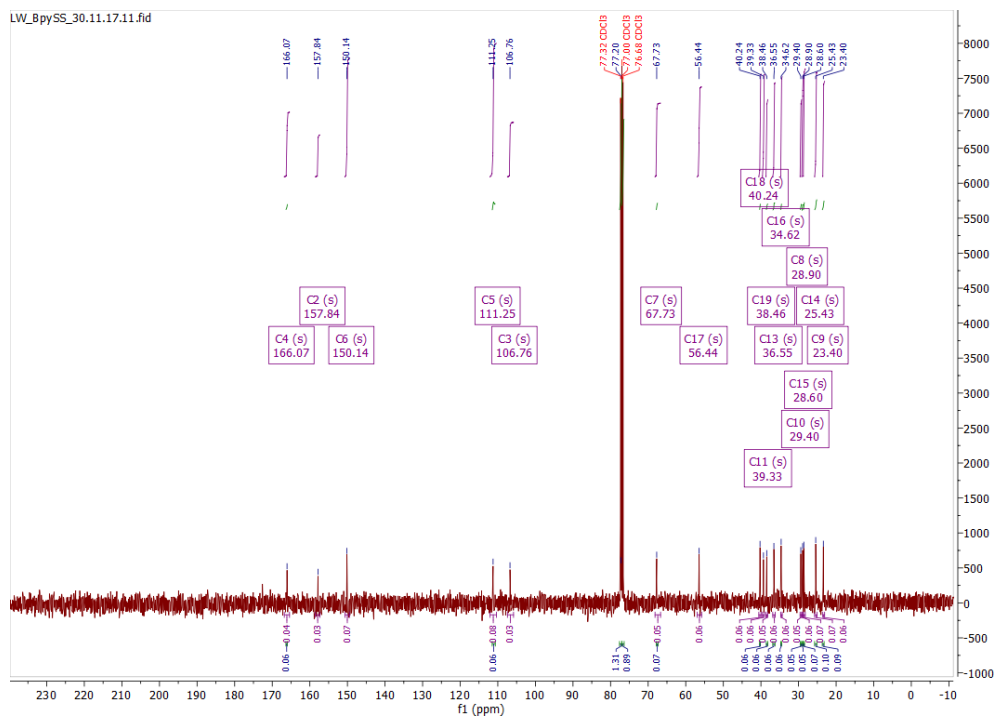


Figure S2. ¹³C NMR spectrum of BpySS in CDCl₃.

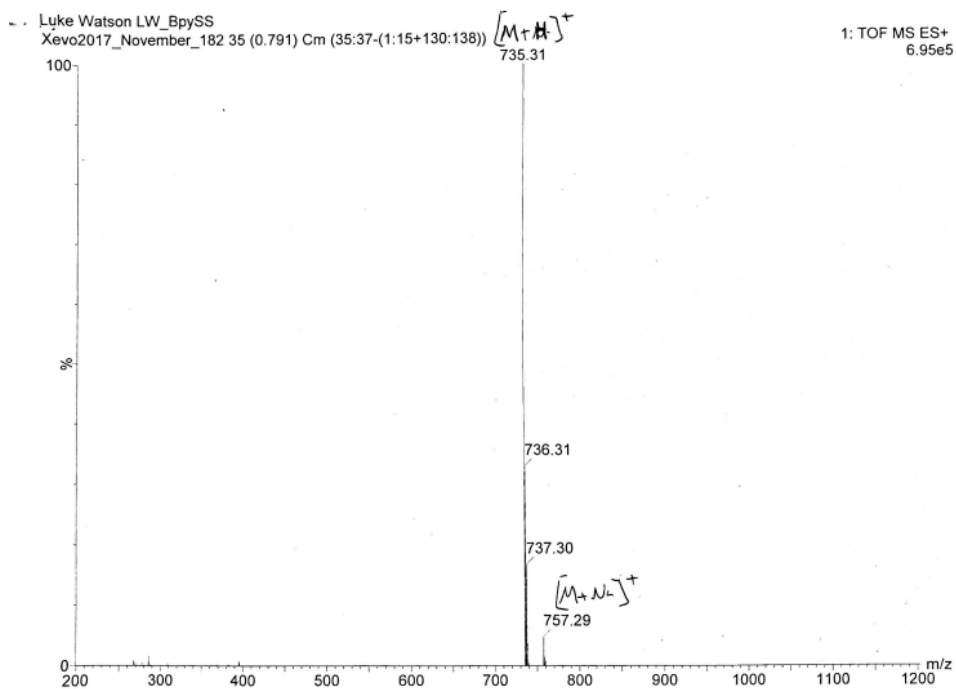


Figure S3. ESI (+) mass spectrum of BpySS.

Os(phen)₂Cl₂ Characterisation

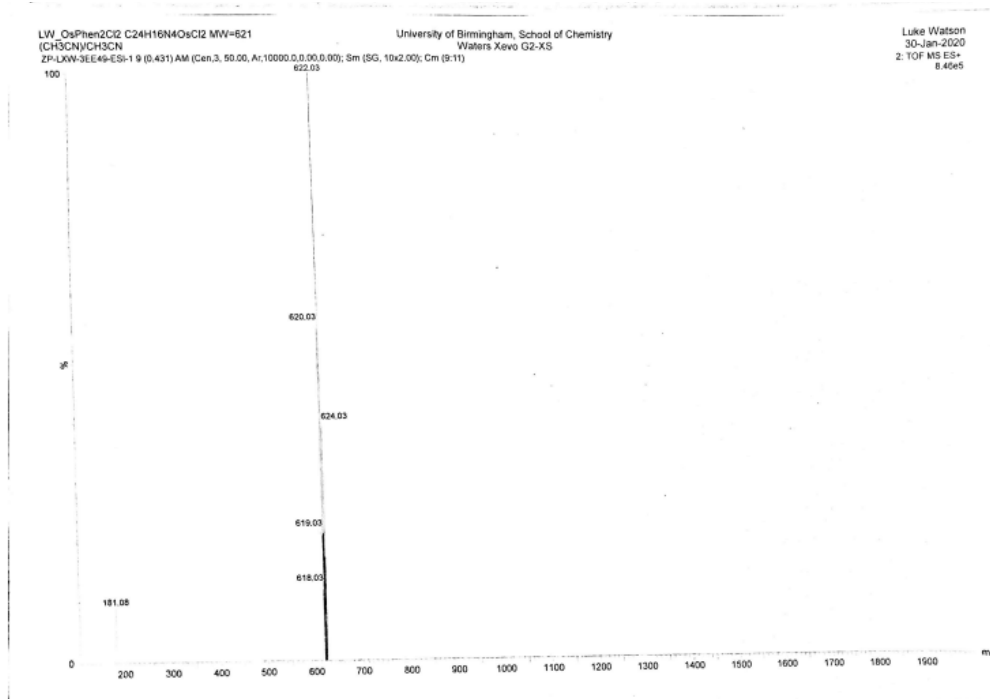


Figure S4. ESI(+) mass spectrum of Os(Phen)₂Cl₂.

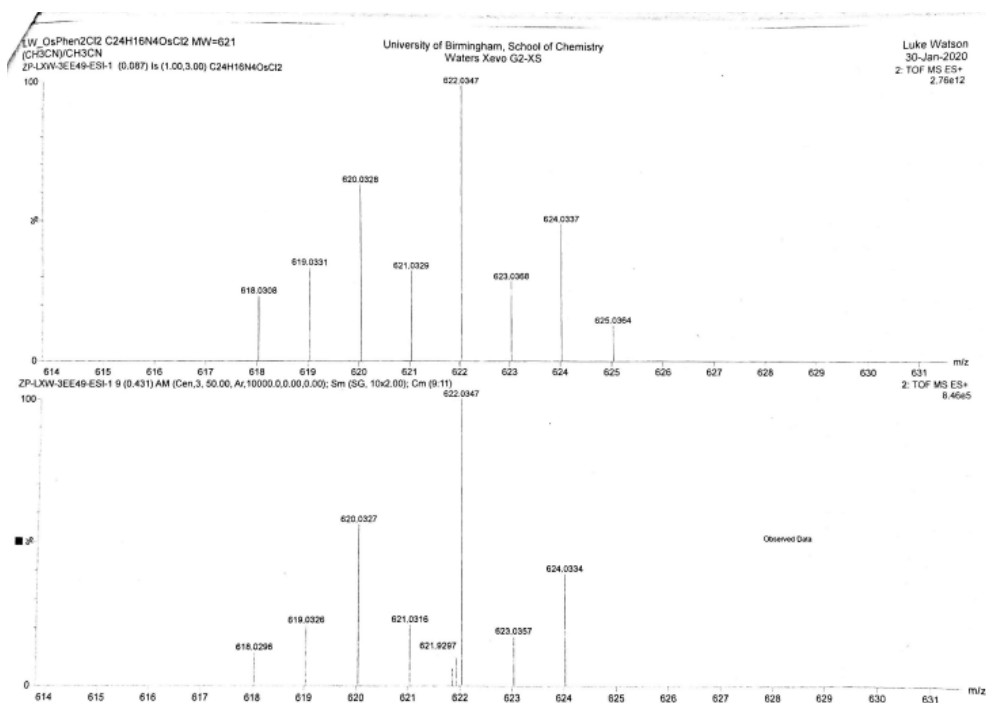
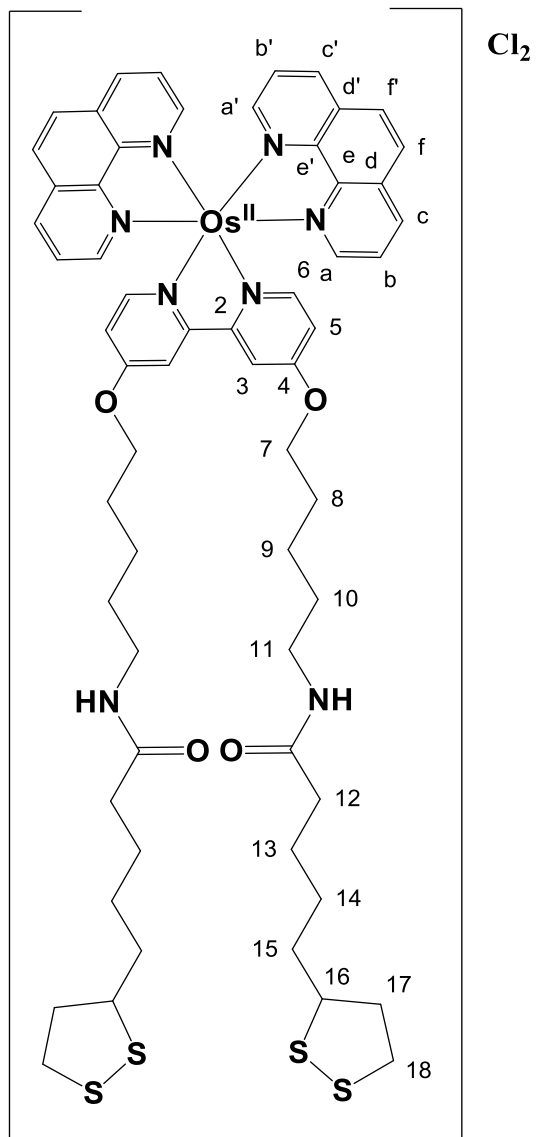


Figure S5. ESI (+) mass spectrum of Os(Phen)₂Cl₂ of experimental mass vs theoretical mass.

OsPhenSS Characterisation



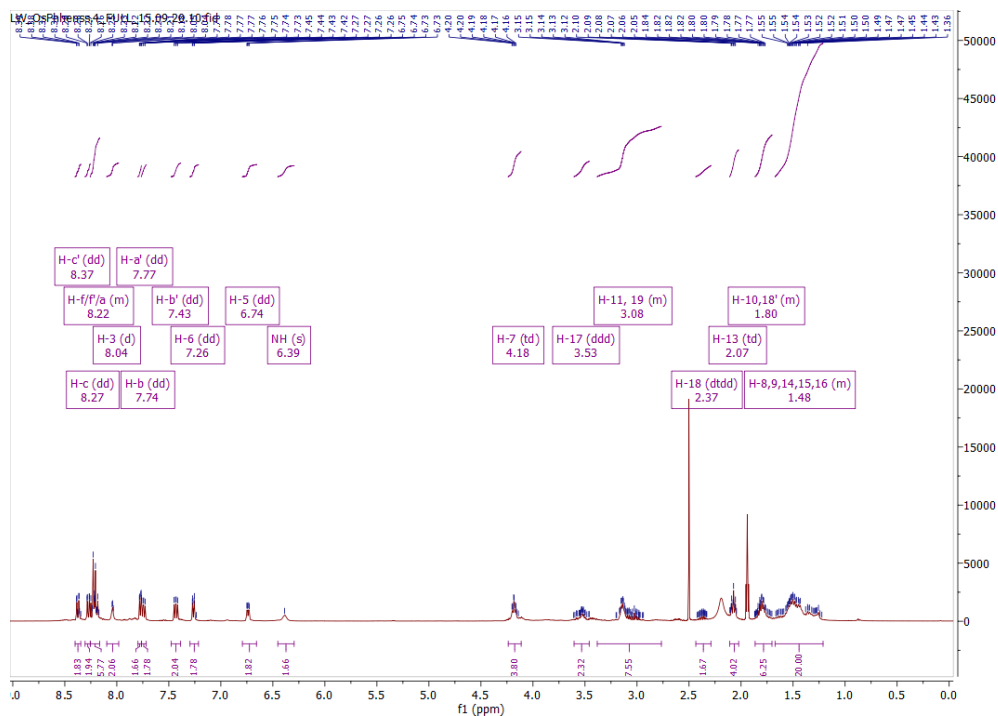


Figure S6. ^1H NMR spectrum of OsPhenSS in CD_3CN .

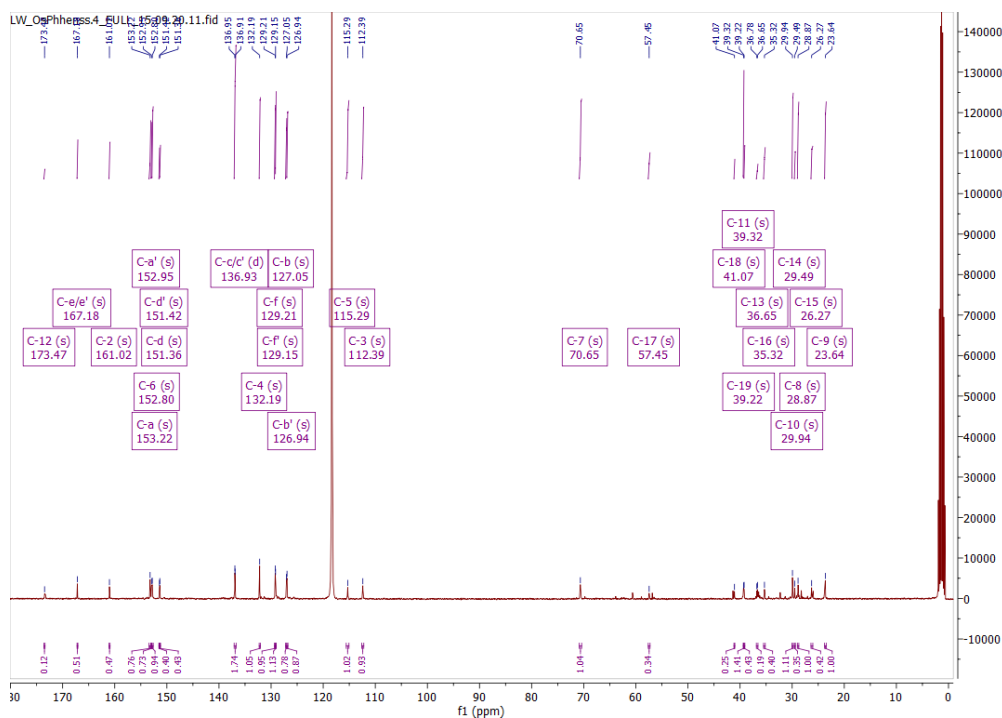


Figure S7. ^{13}C NMR spectrum of OsPhenSS in CD_3CN .

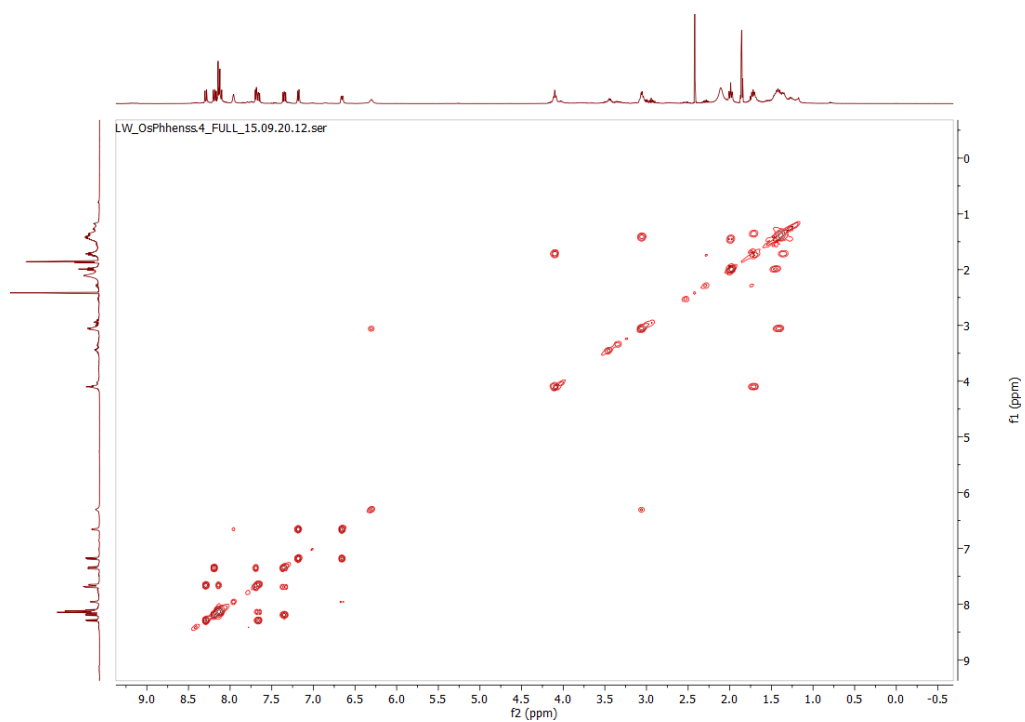


Figure S8. COSY spectrum of OsPhenSS in CD₃CN.

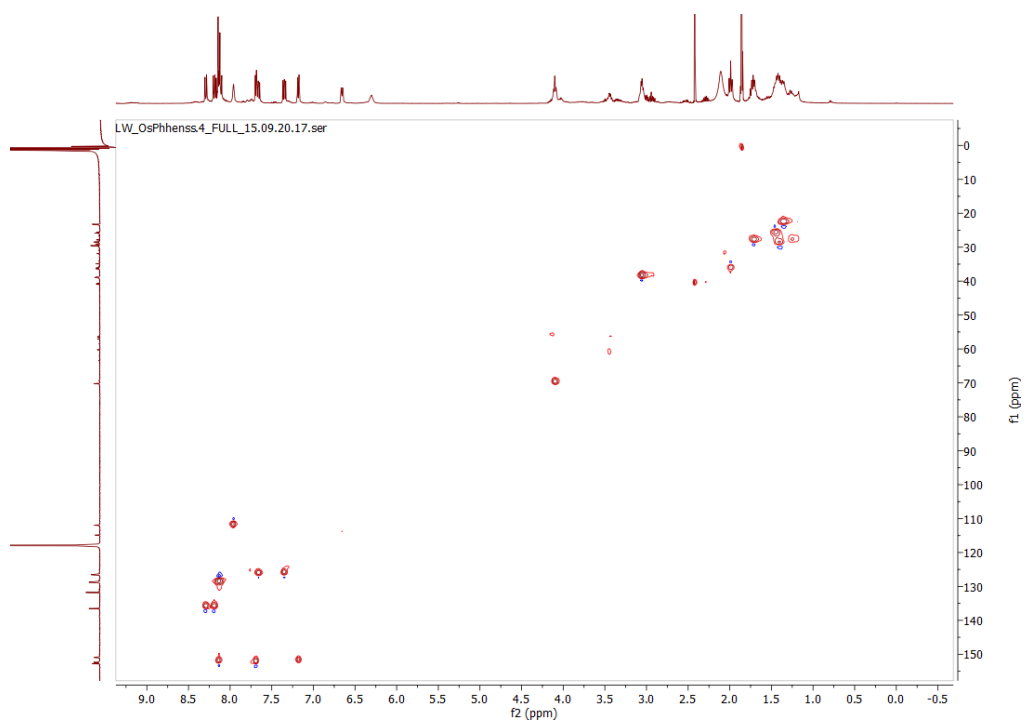


Figure S9. HSQC spectrum of OsPhenSS in CD₃CN.

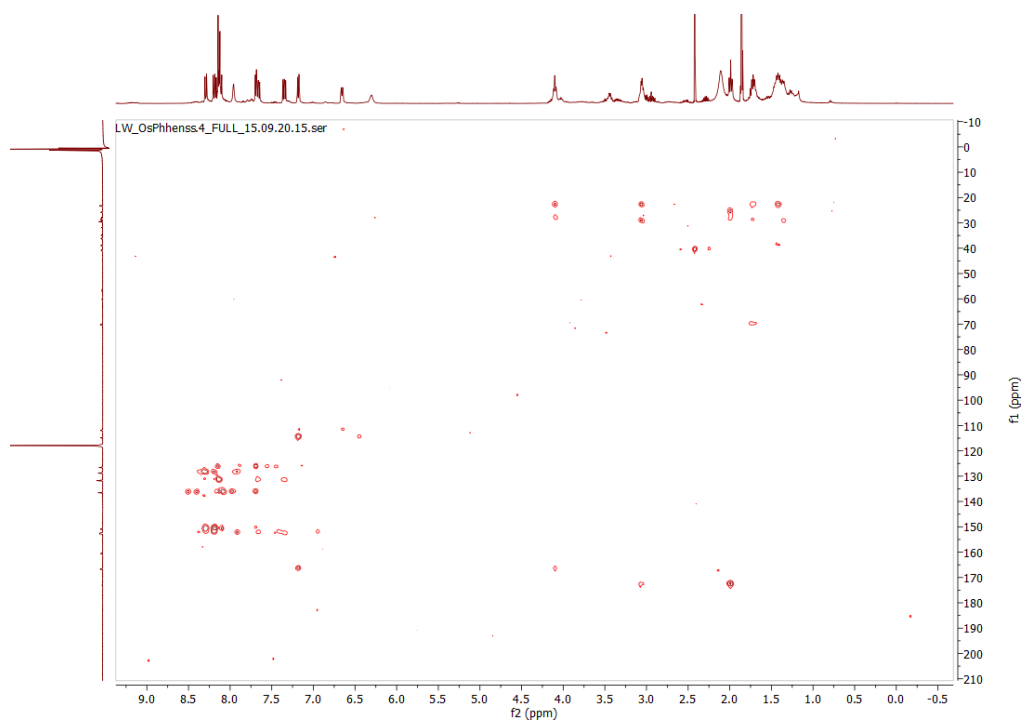


Figure S10. HMBC spectrum of OsPhenSS in CD₃CN.

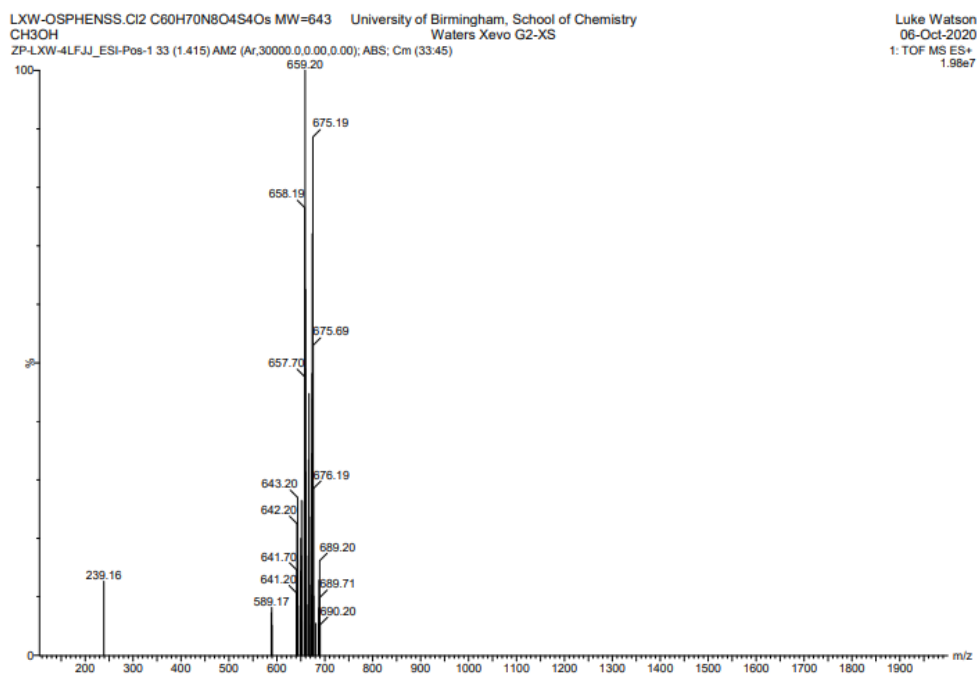


Figure S11. ESI (+) mass spectrum of OsPhenSS.

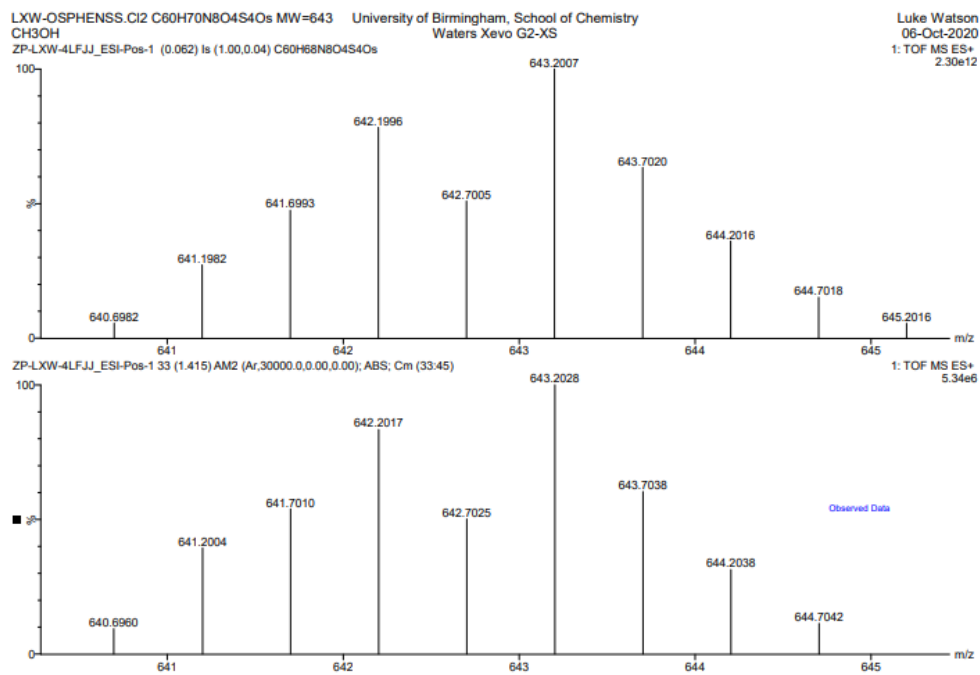


Figure S12. ESI (+) mass spectrum of OsPhenSS. Theoretical mass vs experimental exact mass.

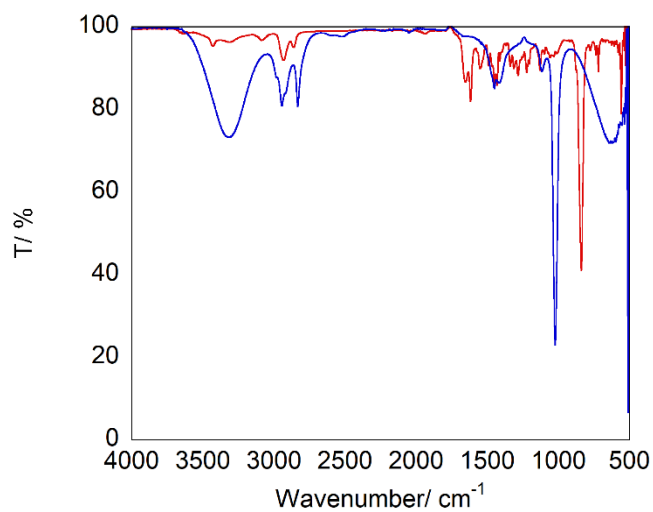


Figure S13. FTIR spectrum of OsPhenSS as the PF₆ counter ion (red) and the Cl counter ion (blue) showing successful ion exchange.

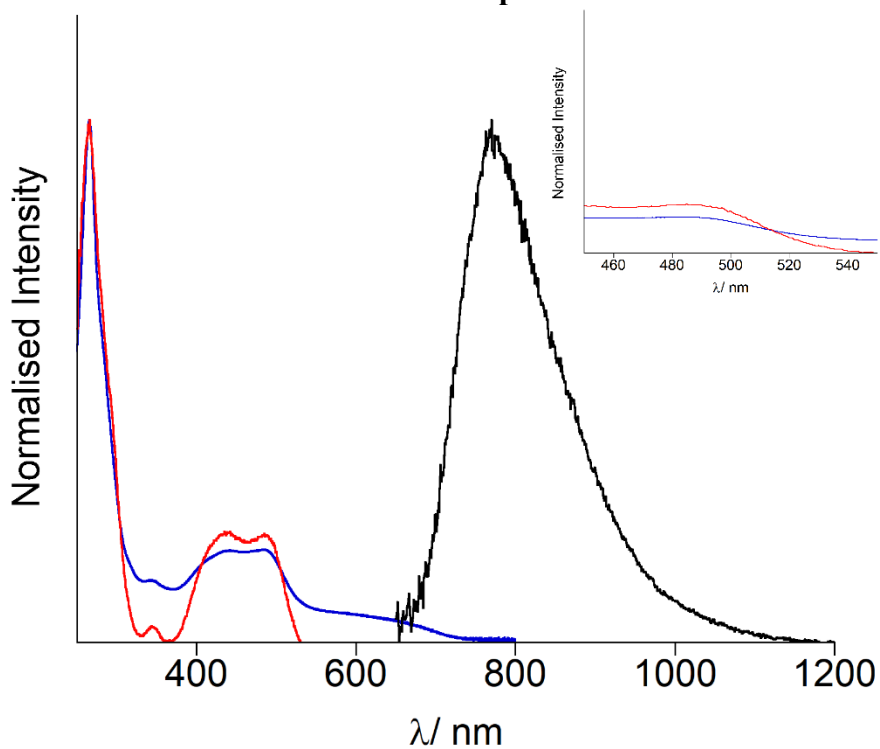
Photophysical Characterisation of OsPhenSS in presence of fluorosurfactant

Figure S14. Normalised emission (black), excitation (red) and UV Vis (blue) of 10 μM **OsPhenSS** in the presence of 485 μM Zonyl FSA in 1mL aerated water ($\lambda_{\text{ex}} = 485\text{nm}$, $\lambda_{\text{em}} = 770\text{nm}$). Insert is magnification of excitation spectra 450 – 550 nm showing tail off.

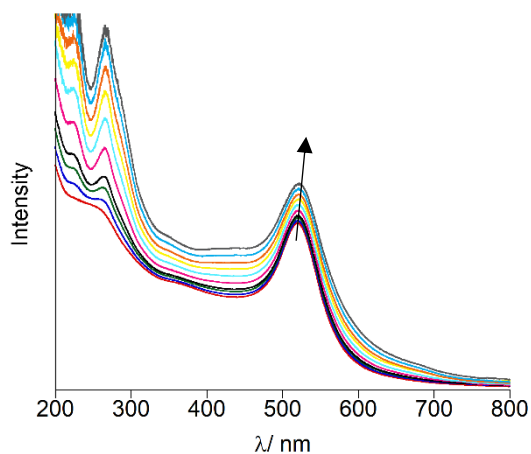


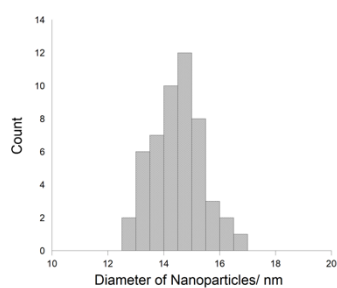
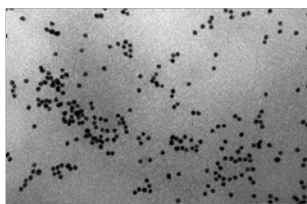
Figure S15. UV-Vis titration of 5 μL quantities of 1 mM **OsPhenSS** into 2 nM **Z•AuNP25** in water (35 μL added).

Data summary of gold nanoparticles' characterisation data

(A)

| | λ_{\max} / nm | Shift / nm |
|------------------------|-----------------------|------------|
| AuNP13 | 517 | 0 |
| Z•AuNP13 | 518 | 1 |
| OsPhenSS•AuNP13 | 521 | 4 |
| AuNP25 | 518 | 0 |
| Z•AuNP25 | 519 | 1 |
| OsPhenSS•AuNP25 | 524 | 6 |

(B)



(C)

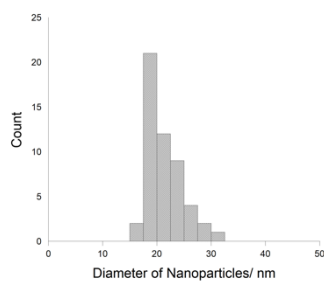
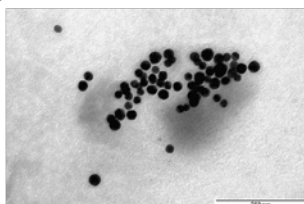


Figure S16. (A) Summary of UV-Vis shifts of gold nanoparticle samples; TEM images of (B) OsPhenSS•AuNP13 and (C) OsPhenSS•AuNP25 and associated histogram plots (n = 50). Scale bar = 200 nm.

(A)

| | Number/ nm | Volume/ nm | PDI | Zeta potential / mV |
|--|------------|------------|-------|---------------------|
| AuNP13 | 14 ± 3 | 17 ± 4 | 0.06 | -35 ± 4 |
| Z•AuNP13 | 20 ± 5 | 23 ± 5 | 0.12 | -49 ± 5 |
| OsPhen•AuNP13 | 18 ± 5 | 31 ± 14 | 0.27 | -39 ± 8 |
| AuNP25 | 21 ± 5 | 25 ± 7 | 0.07 | -34 ± 4 |
| Z•AuNP25 | 29 ± 8 | 34 ± 13 | 0.26 | -42 ± 4 |
| OsPhen•AuNP25 | 27 ± 8 | 40 ± 25 | 0.32 | -36 ± 3 |
| AuNP13 in D₂O | 13 ± 3 | 16 ± 6 | 0.095 | -32 ± 8 |
| Z•AuNP13 in D₂O | 21 ± 6 | 27 ± 10 | 0.271 | -76 ± 12 |
| OsPhenSS•AuNP13 in D₂O | 22 ± 6 | 28 ± 11 | 0.265 | -36 ± 8 |

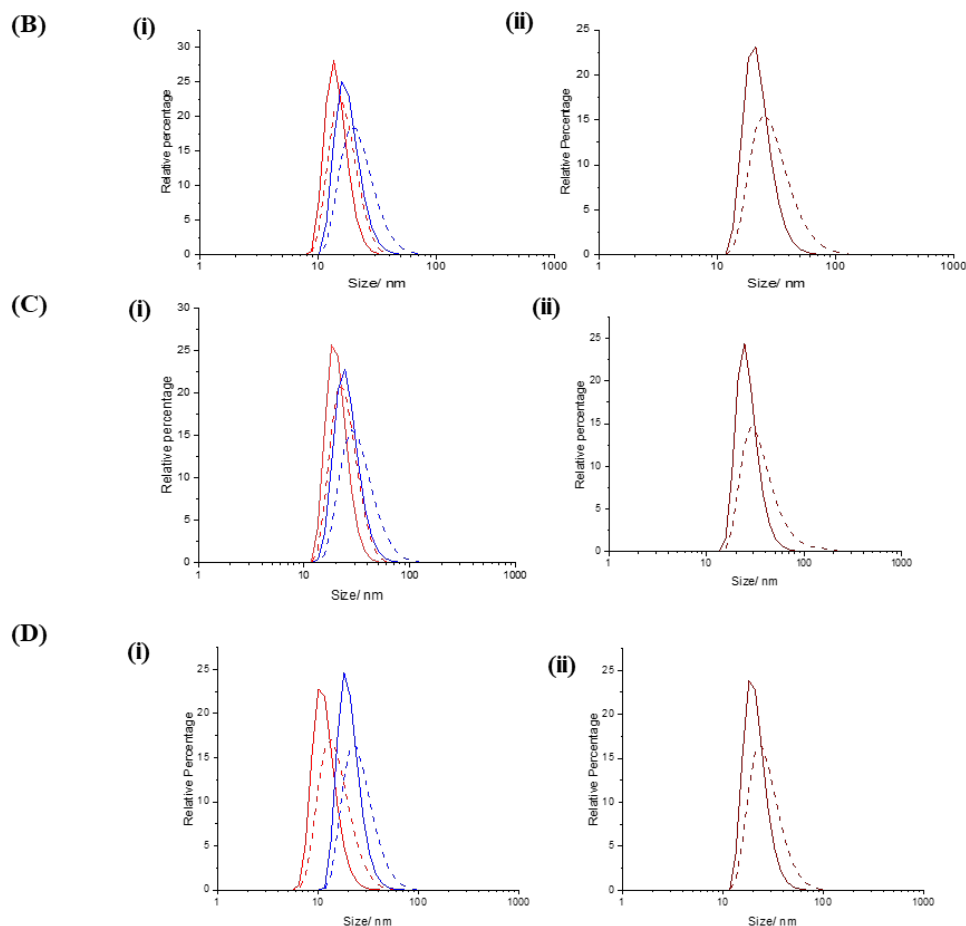


Figure S17. (A) Summary of Dynamic Light Scattering (DLS) data of gold nanoparticle samples ($n = 5$ for size and $n = 3$ for ζ -potential); (B) Number (solid line) an Volume (dashed line) size distributions for (i) citrate-capped **AuNP13** (red) and **Z•AuNP13** (blue) and (ii) **OsPhen•AuNP13** (brown); (C) Number (solid line) an Volume (dashed line) size distributions for (i) citrate-capped **AuNP25** (red) and **Z•AuNP25** (blue) and (ii) **OsPhen•AuNP25** (brown); (D) Number (solid line) an Volume (dashed line) size distributions for (i) citrate-capped **AuNP13** in D₂O (red) and **Z•AuNP13** in D₂O (blue) and (ii) **OsPhen•AuNP13** in D₂O (brown).

Photophysical characterisation of OsPhenSS•AuNP25

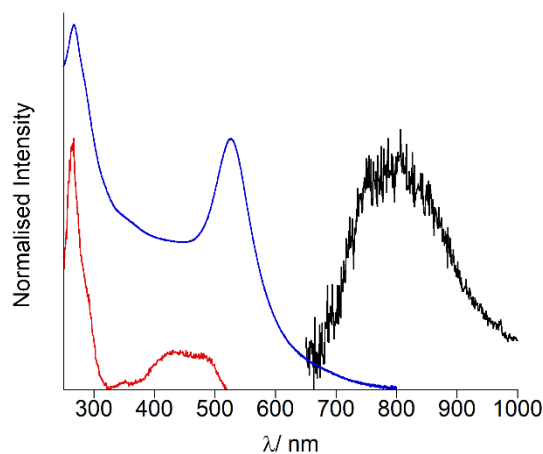


Figure S18. Normalised emission (black, $\lambda_{exc} = 485$ nm), excitation (red, $\lambda_{em} = 785$ nm) and UV-Vis (blue) spectra of **OsPhenSS•AuNP25** (2 nM) in aerated water.

Cell viability assays of OsPhenSS•AuNP in live A549 cells

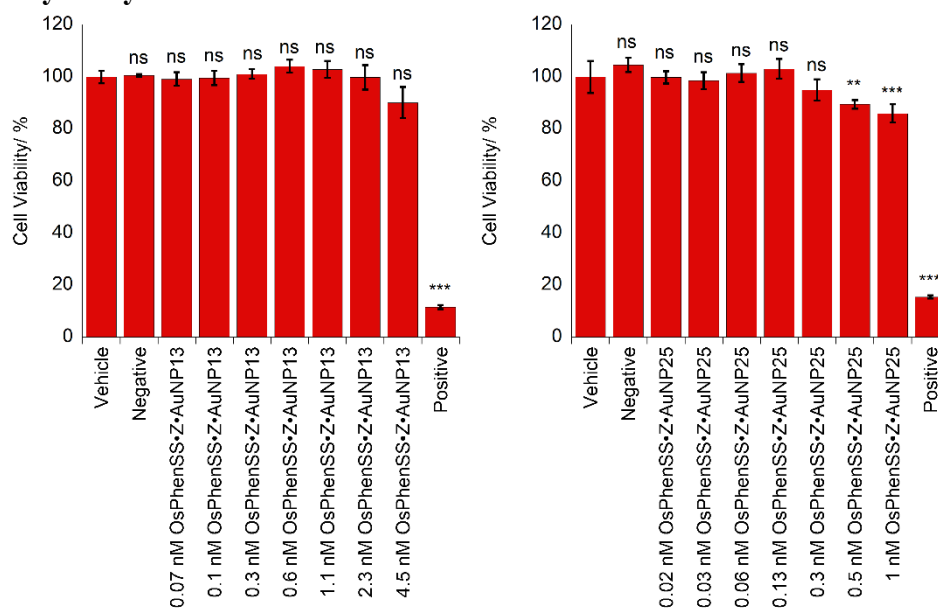


Figure S19. MTT assays of A549 cells treated with serial particle dilutions of (a) **OsPhenSS•AuNP13** and (b) **OsPhenSS•AuNP25** for 24 hours at 37°C 1-way ANOVA followed by a Dunnett's t-test corrected for multiple comparisons. *= $P < 0.05$, **= $P < 0.01$, ***= $P < 0.001$, $n = 3$.

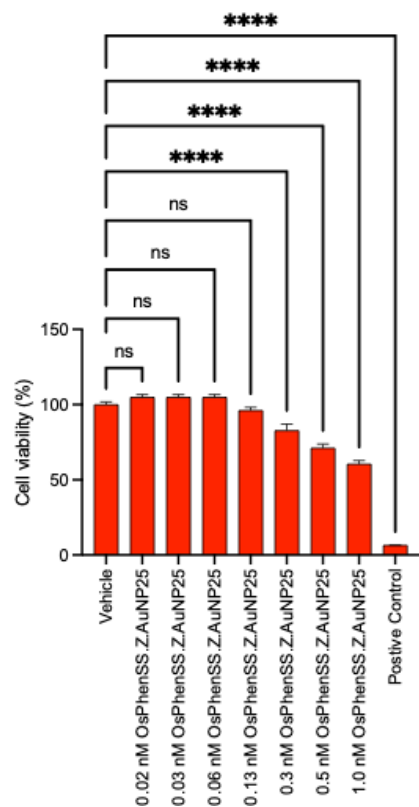


Figure S20. MTT cytotoxicity assay of MRC5 cells (embryonic human lung fibroblasts) treated with **OsPhenSS•AuNP25** for 24 h. Data is plotted as percentage control relative to vehicle alone. As a positive control cells were treated with 0.1% w/v Triton-X-100 for 24 h. The results represent the mean \pm SEM of six technical replicates. ****, statistically significant from vehicle control as assessed by a one-way ANOVA followed by a Dunnett's post-hoc t-test corrected for multiple comparisons, $P < 0.0001$.

Additional Confocal microscopy images of OsPhenSS•AuNP25

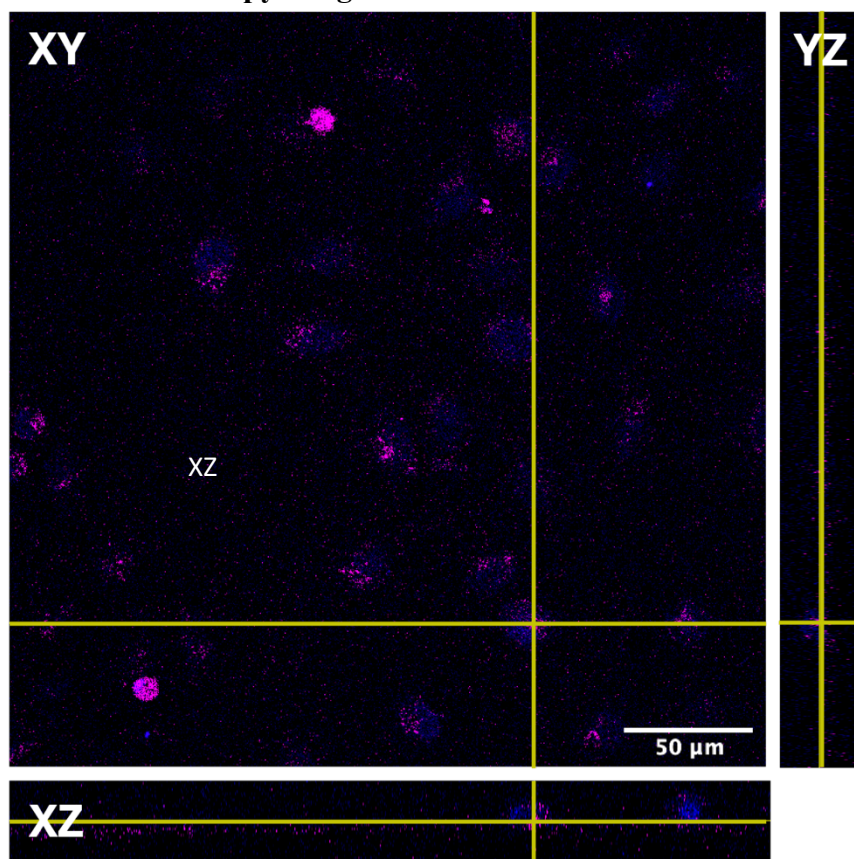


Figure S21. Orthogonal reconstruction of selected central plane from z-stack images of A549 cells showing osmium signal inside cells after incubation with 0.2 nM OsPhenSS•AuNP25 for 18 h at 37°C. Purple channel, osmium emission ($\lambda_{\text{exc}} = 488 \text{ nm}$, $\lambda_{\text{em}} = 650 - 800 \text{ nm}$); blue channel, Hoescht 3368 nuclear staining ($\lambda_{\text{exc}} = 402 \text{ nm}$, $\lambda_{\text{em}} 420-470 \text{ nm}$).

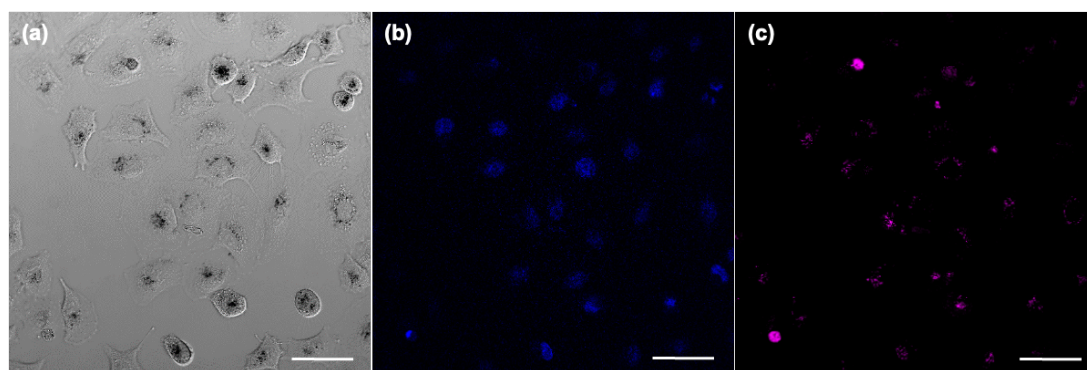


Figure S22. Separate channels (Figure 5) in the live cell images of A549 cells incubated with OsPhenSS•AuNP25 (0.2 nM, incubation for 18 h). (a) brightfield, (b) blue channel, Hoescht 3368 nuclear staining ($\lambda_{\text{exc}} = 405 \text{ nm}$, $\lambda_{\text{em}} = 420 - 470 \text{ nm}$), (c) purple channel, osmium-based emission ($\lambda_{\text{exc}} = 488 \text{ nm}$, $\lambda_{\text{em}} = 650-800 \text{ nm}$). Scale bar is 50 μm .

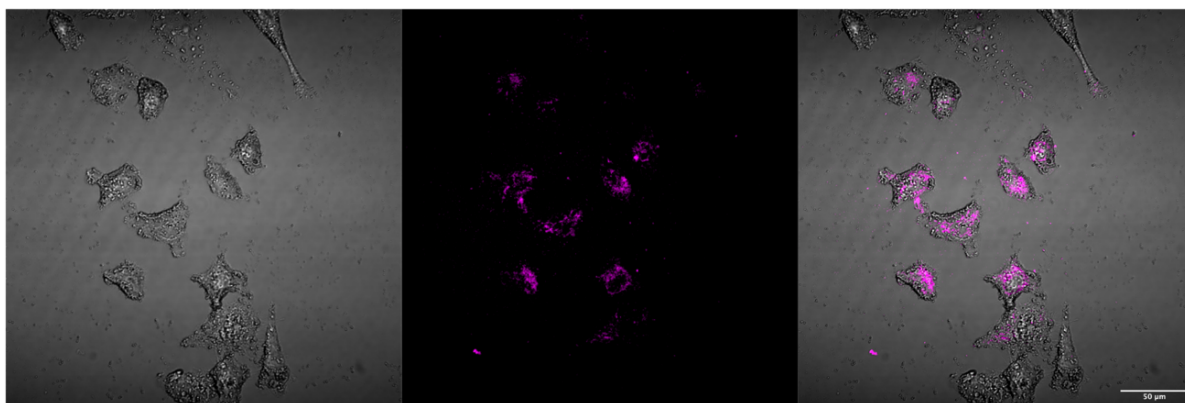


Figure S23. Confocal microscopy of **OsPhenSS•AuNP25** in fixed A549 cells (0.2 nM **OsPhenSS•AuNP25** at 4 h). Brightfield (left); Purple channel, **OsPhenSS•AuNP25** emission ($\lambda_{exc} = 488$ nm, $\lambda_{em} = 650-800$ nm) (middle) and overlap of brightfield and osmium emission (right). Scale bar is 50 μ m.

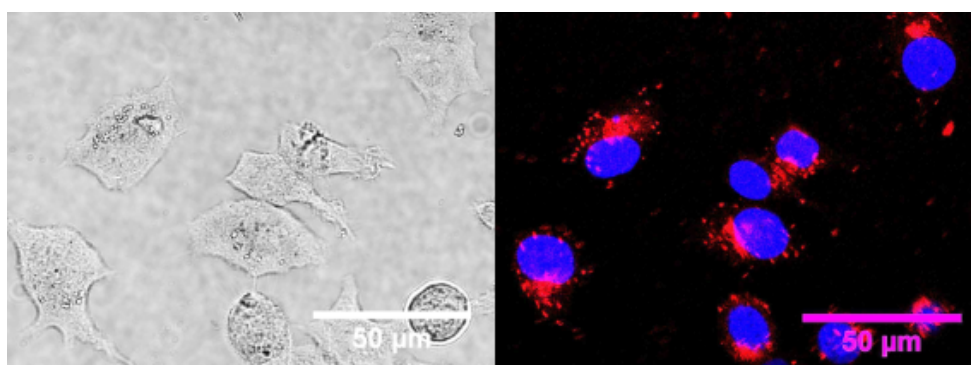


Figure S24. Dual channel fluorescence image of MCF-7 cells with corresponding brightfield image incubated with **OsPhenSS•AuNP25** at 0.1 nM incubated for 24 h (red channel, $\lambda_{exc} = 552$ nm, $\lambda_{em} = 680-710$ nm) and Nuclear Violet (Cambridge Bioscience, UK) incubated for 1 h at 10 μ M prior to imaging (blue channel, $\lambda_{exc} = 405$ nm, $\lambda_{em} = 430-470$ nm) to stain the nucleus. The luminescence shows punctate intracellular and perinuclear distribution. Scale bar is 50 μ m.

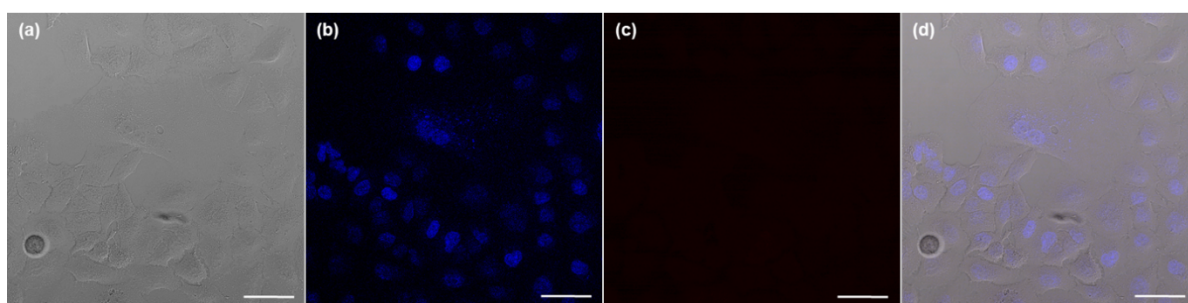


Figure S25. Confocal image of untreated control A549 cells. (a) Brightfield, (b) blue channel, Hoechst 3368 nuclear staining ($\lambda_{exc} = 405$ nm, $\lambda_{em} = 420 - 470$ nm), (c) purple channel, osmium ($\lambda_{exc} = 488$ nm, $\lambda_{em} = 650 - 800$ nm) and (d) overlap of brightfield, blue channel (Hoechst 3368) and purple channel (osmium). Scale bar is 50 μ m.

Calculation of number (N) of gold atoms per nanoparticle

Assuming the gold nanoparticles are perfect spheres and atoms are packed in a uniform face-centred cubic crystalline structure, and taking the density of gold as $\rho_{\text{gold}} = 19.32 \text{ g cm}^{-3}$

$$N = \frac{\rho \times \pi D^3}{6 \times M_r} \times N_A$$

Where M_r of gold = $196.96657 \text{ g mol}^{-1}$, Avogadro's constant $N_A = 6.022140857 \times 10^{23} \text{ mol}^{-1}$

The equation simplifies:

$$N = 30.8969 \times D^3$$
